Yu, J Material Sci Eng 2016, 5:5
DOI: 10.4172/2169-0022.1000278

Journal of Material Sciences & Engineering

Review Article
Open Access

Microstructure Evolution and Brazing Mechanism of Ti_2SnC-Ti_6Al_4V Joint by Using Cu Pure Foil

Yu W*

School of Material Science and Engineering, Tsinghua University, China

Abstract

The MAX phase Ti_2SnC was successfully welded to Ti_6Al_4V (TC_4) through Cu interlayer in Ar atmosphere at low temperature 750°C, during 1h under an applied mechanical pressure 10 MPa. The results indicated that the outward diffusion of Sn from Ti_2SnC played a critical role in the chemical composition of joints. After 60 mins, the reaction layers consist of five zones: interleaved β-Cu(Sn) and α-Cu(Sn) zone zone (V), enriched Sn and $CuTi_{0.5}Sn_{0.5}$ intermetallic phase (IV), poor Sn, Ti and rich Cu zone (III), Ti_3Cu_4 intermetallic (II) and *β*-Ti (Cu) phase (I). Shear test results showed that the average shear strength reached 85.7 ±10 MPa. Corresponding fractographs indicated that the crack mainly propagated along Ti_2SnC substrate adjacent to the bonding zone, accompanied with an intergranular fracture mode.

Keywords: Dissimilar welding; Interfacial diffusion; Shear strength

Introduction

TC4–based alloys are attractive candidates for many industries due to their high resistance to corrosion, high strength-to-density ratio and biocompatibility [1]. However, due to the biotoxicity of vanadium element, TC4 has limited biomedical applications. In recent years, extensive investigations have focused on the unique nanolaminate ternary MAX phases (M for early transition metal, A for A-group element, and X for either carbon or nitrogen), because of their combination of metal-like and ceramic-like properties, especially high modulus and corrosion resistance [2-4]. It has been demonstrated that MAX phases are able to restore mechanical damages by crack healing similarly to a biological healing process [5]. For example, MAX phases, such as Ti_3AlC_2 and Ti_2AlC, could heal millimeter-sized cracks through the formation of intermediate solid phases resulting from the oxidation of the diffused A-element (Al, Sn) [3,6-8]. Therefore, diffusion bonding is considered highly applicable for MAX phases. For example, Li et al. showed that strong joints of Ti_3AlC_2 can be achieved at 1400°C with the preferential oxidation form of Al_2O_3 layer through the whole joint interface [9]. Gao and Miyamoto conducted the diffusion bonding of Ti_3SiC_2 with TC4 in the temperature range from 1200°C to 1400°C, and the bending strength of the joints was 100MPa ± 20MPa when joined at 1350°C for 1 h. The fracture occurred in the $Ti_5Si_3C_x$ single layer at the interface [10]. Recently, Yin et al. successfully welded Ti_3SiC_2 and TiAl through a Ni foil at 1000°C [11]. In summary, these studies were carried out above 1000°C and the addition of Ni interlayer could significantly decrease the joining temperature.

As one of the most attractive MAX phases, the Sn atoms in Ti_2SnC begin to diffuse out at 700°C in crack healing experiments [12]. Copper has a good compatibility with TC4 and Cu-Sn alloy becomes liquid above 730°C when the ratio of Cu: Sn is under 3:1 in Cu-Sn phase diagram [13]. Herein, the diffusion bonding and reactivity between TC4 and Ti_2SnC through the Cu interlayer were investigated in this work, which could promote potential application of these new materials.

Experimental Procedure

The chemical composition of TC4 material was: Ti: Base, Al: 6.5%, V: 3.7%, Fe: 0.18% in wt%. Bulk Ti_2SnC was prepared by hot pressing a mixture of Ti, Sn, C powders with a molar ratio of 2:1:1 at 1250°C under an applied pressure of 30 MPa during 60 min in vacuum. Specimens were cut from the bulk materials by electrical discharge machine with cylindrical dimensions of φ12 mm × 4 mm and φ8 mm × 5 mm for TC4 and Ti_2SnC, respectively (Figure 1). The interlayer material used in this study was pure Cu foil (99.9%, 50 µm). Finally, the pellets sandwiches of TC_4/Cu/Ti_2SnC were heated in a High-frequency induction heating device characterized with constant parameters of 6.0 A and 225 kHz. During the heating process, the pellets were heated to 750°C under Ar atmosphere with an applied pressure 5MPa at constant heating rate of 20°C/s, as shown in Figure 1b.

In this work, scanning electron microscopy (Zeiss Merlin Germany) and electron probe micro-analyzer (EPMA, JSM-7001f) were adopted investigate the joint microstructure and analyze the chemical composition of different phases. The polished interface was also analyzed by X-ray diffraction. (Cu Kα, Rigaku D/max-2004, japan). The Vickers hardness was determined with a Zwick/Z2.5 hardness tester (Ulm, Germany) in a same load of 1N and at a constant contact time of 15 s.

A specially testing fixture was designed to determine bond shear strength {Torun, 2008 #317}, which was schematically shown in Figure 2. The shear strength test was carried out by a ZWICK-Z020 material test system at a speed of 1 mm/min. The average value for the bonded joints was obtained through measuring 4 samples. Finally, the fracture surface was also observed by scanning electron microscopy.

Results and Discussion

Interfacial microstructure of TC4/Ti_2SnC diffusion bonded joints

Figure 3 presents the interfacial microstructure of the TC4/Ti_2SnC joint using Cu interlayer bonded at 750°C for 60 minutes under 10 MPa. According to the Cu-Sn diagram and EPMA results, it is confirmed that β-Cu(Sn) (bright area, 81.6% Cu and 18.4% Sn in atoms) and α-Cu(Sn) (grey area 91.6% Cu and 8.5% Sn in atoms) are uniformly interleaved

---

***Corresponding author:** Yu W, School of Material Science and Engineering, Tsinghua University, China, Tel: 861062793001; E-mail: wenboyu@tsinghua.edu.cn

Received June 14, 2016; **Accepted** September 02, 2016; **Published** September 12, 2016

Citation: Yu W (2016) Microstructure Evolution and Brazing Mechanism of Ti_2SnC-Ti_6Al_4V Joint by Using Cu Pure Foil. J Material Sci Eng 5: 278. doi:10.4172/2169-0022.1000278

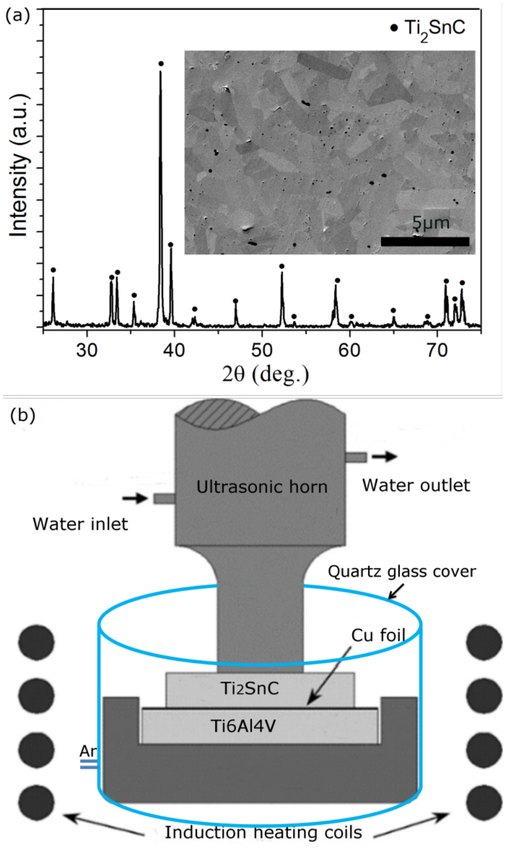

Figure 1: (a) Microstructure and X-ray diffraction result of the bulk Ti_2SnC, (b) Schematic illustration of the experimental assembly.

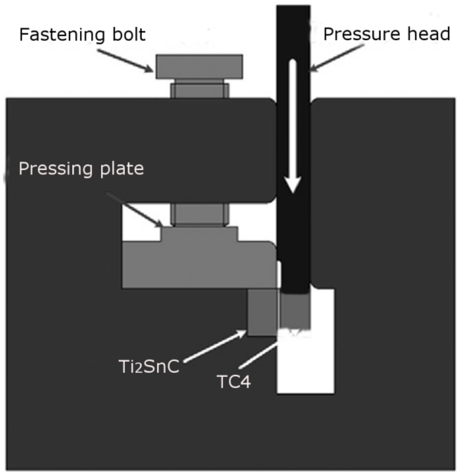

Figure 2: Schematic of shear test.

together in layer (V), as shown in the joint. Furthermore, the variations of the different element in EPMA line analysis suggest that a sound joining of Ti_2SnC to TC4 was achieved. Concerning the TC4 side, the formation of layer I resulted from the atomic migration of Cu into β-Ti titanium due to the more open crystallography in β-Ti [14,15]. Layer II is composed of 51.6% Cu, 43.99% Ti, 2.5% Al and 1.4% V in atomic fraction, supposed to be Ti_3Cu_4. Layer III was characterized with 92.1% Cu, 4.5% Ti, 1.5% Sn, 0016% Al and 1.4% V. Layer IV contained 45.5% Cu, 22.1% Ti, 31.1% Sn, supposed to be $CuTi_{0.5}Sn_{0.5}$ and Sn. On the other side, Figure 3c shows a distinct migration of Sn atoms (bright color) along the grain boundary. According to previous studies, destabilization of the MAX phases crystal lattice tend to release A atoms under 1200°C [2,14]. Especially for Ti_2SnC, the destabilization temperature is as lower as 700°C due to the high mobility of Sn in Ti_2SnC, driven by its low migration energy of 0.66 eV as well as fluid flow transport above its low melting point of 232°C [8,12]. Furthermore, no Ti_2SnC decomposition was found in this work, but the ration between Ti and Sn decreased to be 2:0.91 from the starting ratio 2:1.01 [16-18].

Figures 4a and 4b present the corresponding surface morphologies obtained at 20 and 35 minutes, respectively. The declined Sn curve from the Ti_2SnC to TC4 clearly indicates that outward diffused Sn atoms from Ti_2SnC moved to TC4. With the increasing processing time, the line scan EPMA results show Sn atoms began to accumulate adjacent to TC4 side, as shown in the dotted circles in Figure 4b. Furthermore, the chemical composition of different layers labeled in the insets was summarized in Table 1 [17]. Regardless the processing time, the chemical composition of I II and III layers did not change. However, with the increasing processing time, Sn began to accumulate between layer IV and V. Finally, these two layers became combined into one

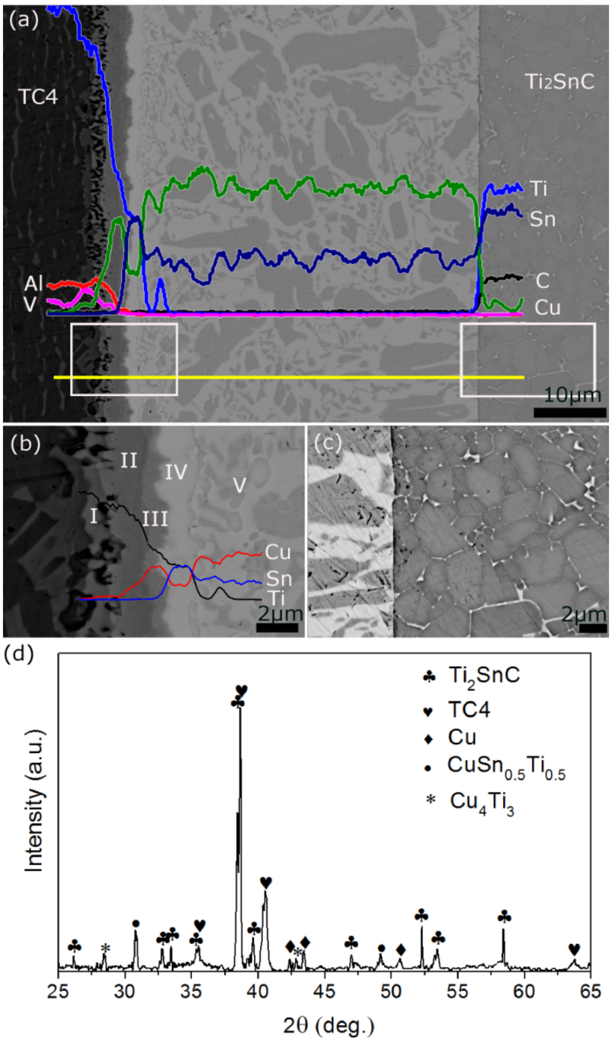

Figure 3: (a) BSE image of the polished surface with result of EPMA for the profiles of constituent elements obtained after 60 mins; (b) and (c) The insets show the magnification image of the reaction zones adjacent to TC4 and Ti_2SnC, respectively; (d) X-ray diffraction pattern of the joint.

single layer, which is an enriched Sn and Ti-Cu-Sn intermetallic phase. Furthermore, based on the increased Ti content from layer I to IV and decreased Sn content from V to II, it can be concluded that the diffusion of Ti into Cu is effective to decrease the activity of Sn [16].

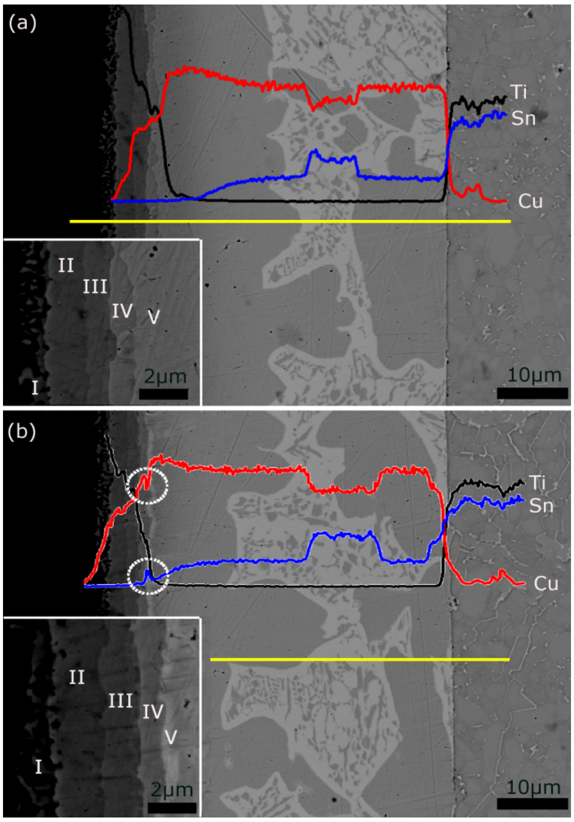

Figure 4: SEM image of the polished surface with result of EPMA for the profiles of constituent elements with different processing time, (a) 20 mins and (b) 35 mins. The insets are the magnification image of the reaction zones adjacent to TC4 side, respectively.

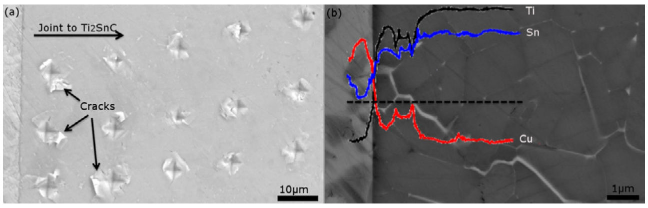

Figure 5: (a) The arrays of indents under Vikers hardness test (b) EPMA analysis for the profiles of constituent elements.

Based on the above analysis, the reaction in $Ti_6AlV/Cu/Ti_2SnC$ bonded joints can be described using the following reaction route. The side adjacent to Ti_2SnC,

$Ti_2SnC \rightarrow xSn + Ti_2Sn_{1-x}C$ (1)

$Sn + Cu \rightarrow \beta\text{-}Cu\ (Sn) + \alpha\text{-}Cu\ (Sn)$ (2)

The side adjacent to TC4, the interdiffusion between Ti and Cu resulted into the following reaction.

$Cu + \beta Ti \rightarrow \beta Ti\ (Cu)$ (layer I) (3)

$3Ti + 5Cu \rightarrow Ti_3Cu_4$ layer (II) + Cu (Sn,Ti) (layer III) (4)

With the increasing processing time, Sn atoms began to accumulate into Cu(Ti) layer and form $CuTi_{0.5}Sn_{0.5}$ intermetallic.

$1.5Sn + Cu\ (Ti) \rightarrow Sn + CuTi_{0.5}Sn_{0.5}$ (layer IV) (5)

Mechanical properties of the Ti_2SnC/Cu/ TC4 diffusion bonded joints

In order to evaluate the influence of diffusion Sn atoms on hardness variations in Ti_2SnC, the hardness test were made along the arrays shown in Figure 5a. Considering about the grains size, several grains are involved in the deformation process. It reveals more cracks happened around the indent corners when the indents are closer to the interfacial joint. This should be attributed to the diffusion of Cu in Ti_2SnC along grain boundaries. Figure 5b shows the variation of Cu curve in Ti_2SnC zone, which indicates that Cu atoms diffused into the Sn liquid along Ti_2SnC grain boundaries. Cu and Sn could form the intermetallic alloy, which is much harder than Sn. Hence, this could strengthen the Ti_2SnC grain boundaries. Herein, the region closed to joint is more rigid than the further zone. Finally, more cracks happened around the indent corners in this region.

The joining properties of the diffusion bonded joints performed at 750°C for 60 minutes were also evaluated via shear strength test. The shear strength of the joint was 85.7 ±10 MPa. In Figure 6a, the brittle intergranular fracture is dominant, only a few grains with delamination of the nano-laminar structure after shear test. This fracture behavior is different from diffusion bonding of Ti_3SiC_2/Ni/TiAl obtained at 1000°C for 60 mins, in which the delamination, kink bands, crack deflection are prevalent [11]. As reported in the literature, MAX phases with fine grain size have a much higher hardness and young's modulus than those with coarse grain size [15,16]. Herein, bonding interface has higher strength in our work than that (52.3 MPa) of Ti_3SiC_2/Ni/TiAl [11]. Furthermore, the Sn traces (bright color) can be found along the grain boundaries presented in Figure 6b, which confirms the Sn diffusion out of Ti_2SnC matrix. The joining of TC4 to Cu-10Sn was effectively achieved by

Label	Elements Time (mins)	Sn atoms%	Cu atoms%	Ti atoms%	Al atoms%	V atoms%	Possible phases
I	Any time	0	2.7	92.4	3.1	1.8	βTi(Cu)
II	Any time	0.6	51.6	43.99	2.5	1.4	Ti_3Cu_4
III	Any time	1.5	92.1	4.5	1.6	0.3	Poor Sn rich Cu
IV	20 mins	2.1	93.8	2.8	0.8	0.5	
	35 mins	5.8	87.3	5.2	0.9	0.8	
V	20 mins	8.7	84.5	5.3	0.8	0.7	
	35 mins	14.7	73.7	10.2	0.9	0.5	
IV and V	60 mins	31.1	45.5	22.1	0.7	0.6	Rich Sn $CuTi_{0.5}Sn_{0.5}$

Table 1: Summary of the different layers chemical compositions as labeled in the insets with different processing times.

Citation: Yu W (2016) Microstructure Evolution and Brazing Mechanism of Ti_2SnC-Ti_6Al_4V Joint by Using Cu Pure Foil. J Material Sci Eng 5: 278. doi:10.4172/2169-0022.1000278

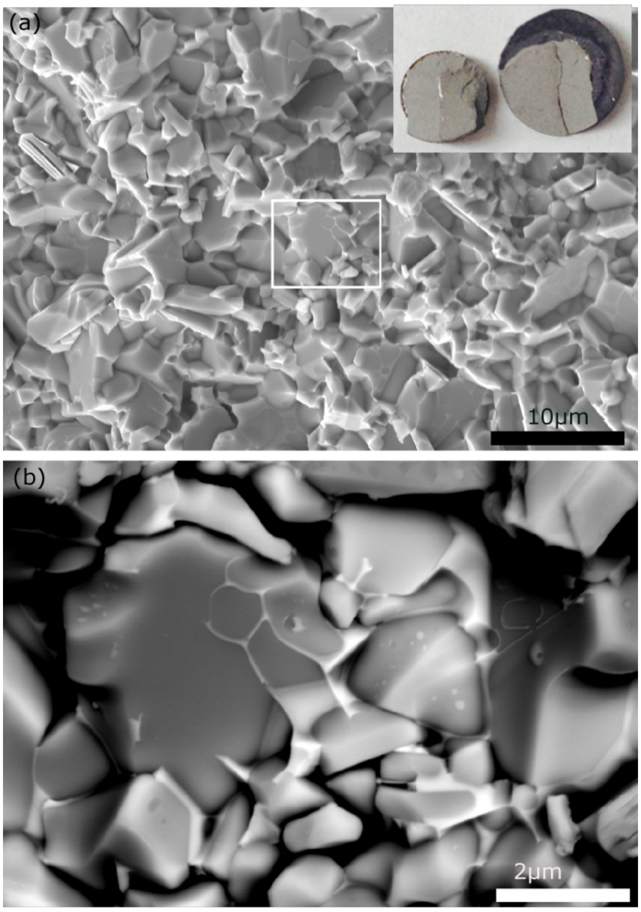

Figure 6: (a) Secondary electron image of fracture of the Ti_2SnC/Cu/ TC4 bonded joint at 750ºC for 60 minutes under 10 MPa. (b) The inset is the backscattered electron image of the enlarged area marked in (a).

diffusion bonding method. When the joint was attached at 830℃ for 15 min, the highest shear strength (102 MPa) was obtained.

Conclusions

Dissimilar welding of Ti_2SnC and TC4 has been successfully performed in Ar atmosphere at relative low temperature (750ºC) using Cu foil as interlayer under 10 MPa. The results demonstrated that Sn can diffuse out along grain boundaries from Ti_2SnC and into Cu foil. With the increasing processing time, Sn atoms migrated and accumulated adjacent to TC4 side as diffusion of Ti into Cu-Sn is effective to decrease the activity of Sn. After 60 mins, the reaction layers consist of five zones: interleaved β-Cu(Sn) and α-Cu(Sn) zone zone (V), enriched Sn and $CuTi_{0.5}Sn_{0.5}$ intermetallic phase (IV), poor Sn, Ti and rich Cu zone (III), Ti_3Cu_4 intermetallic (II) and β-Ti (Cu) phase (I). Shear test results showed that the maximum shear strength reached 85.7±10 MPa. Corresponding fractographs indicated that the crack mainly propagated along Ti_2SnC substrate adjacent to the bonding zone, accompanied with a brittle intergranular fracture mode.

Acknowledgements

This work was financially support by the class General Financial Grant from the China Postdoctoral Science Foundation (2015M580093).

References

1. Barsoum MW (2000) The MN+1AXN phases: a new class of solids; thermodynamically stable nanolaminates. PROG SOLID STATE CH 28: 201-281.
2. Barsoum M, El-Raghy T (1996) Synthesis and characterization of a remarkable ceramic: Ti_3SiC_2. J Am Ceram Soc 79: 1953-1956.
3. Wang X, Zhou Y (2003) High-temperature oxidation behavior of Ti_2AlC in air. Oxidation of Metals 59: 303-320.
4. Barsoum M, Brodkin D, El-Raghy T (1997) Layered machinable ceramics for high temperature applications. Scripta Materialia 36.
5. El-Raghy T, Blau PJ, Barsoum M (2000) Effect of grain size on friction and wear behaviour of Ti_3SiC_2. Wear 238: 125-130.
6. Gupta S, Filimonov D, Palanisamy T, Barsoum M (2008) Tribological behavior of select MAX phases against Al_2O_3 at elevated temperatures. Wear 265: 560-565.
7. Oh CS, Han CS (2012) Retracted article: Precipitation behavior of Al-Ti-Ag alloy system. Met Mater Int 18: 397.
8. Kuisma-Kursula P (2000) Accuracy, precision and detection limits of SEM-WDS, SEM-EDS and PIXE in the multi-elemental analysis of medieval glass. X-Ray Spectrometry 29: 111-118.
9. Wang J, Zhou Y, Liao T, Lin Z (2008) A first-principles investigation of the phase stability of Ti_2AlC with Al vacancies. Scripta Materialia 58: 227-230.
10. Kaur I, Gust W (1989) Handbook of grain boundary and interface boundary diffusion data. Ziegler Press, Stuttgart.
11. Bard AJ, Faulkner LR (1980) Electrochemical methods: fundamentals and applications. Wiley, New York.
12. Moon KW, Williams ME, Johnson CE, Stafford GR, Handwerker CA, et al. (2001) Proceedings of the Fourth Pacific Rim Conference on Advanced Materials and Processing.
13. Wang J, Li Y, Liu P, Geng H (2008) Microstructure and XRD Analysis in the interface zone of Mg/Al diffusion bonding. J Mater Process Technol 205: 146-150.
14. Tomiharu O (2004) Resistance welding of aluminum alloy to dissimilar metals. J Light Metal Weld Const 42: 2-15.
15. Mahendran G, Balasubramanian V, Senthilvelan T (2009) Developing diffusion bonding windows for joining AZ31B magnesium-AA2024 aluminium alloys. Mater Des 30: 1240-1244.
16. Yeh MS, Chuang TS (1995) Low pressure diffusion bonding of SAE 316 stainless steel by inserting a super plastic interlayer. Scripta Metall Mater 33: 1277-1281.
17. Liu P, Li YJ, Geng HR, Wang J (2005) A study of phase constitution near the interface of Mg/Al vacuum diffusion bonding. Mater Lett 59: 2001-2005.
18. Mahendran G, Balasubramanian N, Senthilvelan T (2010) Influences of diffusion bonding process parameters on bond characteristics of Mg-Cu dissimilar joints. Trans NonFerrous Met Soc China 20: 997-1005.